ISSN 2079-1704. Хімія, фізика та технологія поверхні. 2023. Т. 14. № 2. С. 210-222

UDC 669.25 : 620.18 doi: 10.15407/hftp14.02.210

Z.A. Matysina [1], An.D. Zolotarenko [1, 2], Ol.D. Zolotarenko [1, 2], T.V. Myronenko [1], D.V. Schur [1, 4], E.P. Rudakova [1, 2], M.V. Chymbai [1, 2], A.D. Zolotarenko [1], I.V. Zagorulko [3], O.O. Havryliuk [2]

EMBEDDED ATOMS IN A CRYSTALLINE HEXAGONAL STRUCTURE

[1] Frantsevich Institute for Problems of Materials Science of National Academy of Sciences of Ukraine
3 Krzhizhanovskogo Str., Kyiv, 03142, Ukraine, E-mail: a.d.zolotarenko@gmail.com
[2] Chuiko Institute of Surface Chemistry of National Academy of Sciences of Ukraine
17 General Naumov Str., Kyiv, 03164, Ukraine, E-mail: o.d.zolotarenko@gmail.com
[3] G.V. Kurdyumov Institute for Metal Physics of National Academy of Sciences of Ukraine
36 Academician Vernadsky Blvd., Kyiv, 03142, Ukraine
[4] Institute of Applied Physics of National Academy of Sciences of Ukraine
58 Petropavlivska Str., Sumy, 40000, Ukraine

As part of the work, the hexagonal structure of B19 type metals as hydrogen sorbents will be considered. That is, crystal lattices are considered, where atoms of impurities (hydrogen) are introduced into the interstices of the metal. To do this, we present an image of the B19 structure itself. In this work, the solubility of hydrogen in the crystal structure of B19 type metals was studied using the configuration method, and the dependence on the composition of the alloy and temperature was found in the substitution of nodes and interstices. Also, in the work the degrees of long-range order at the nodes are considered and the parameters of the correlation in the substitution are determined. A graphical view of the effect of atomic order on the solubility of impurities is given. The calculated data obtained in the work coincide with the experimental data of other studies, and the obtained calculation formulas make it possible to determine the energy parameters of the alloys, which is a certain scientific value of the work. The proposed system takes into account only atomic interaction and absorption (dissolution) and diffusion of interstitial atoms into the bulk of the crystal structure; therefore, it is possible to predict the introduction of only a hydrogen atom. Thus, the results obtained in the work of the correlation parameters for the distribution of atoms only in octapores or only in tetrapores allow a deeper study of the physical characteristics of alloys of the B19 type and an understanding of the processes of hydrogen sorption by the working bodies of hydrogen storage.

***Keywords**: Hydrogen, metal, alloys, solubility, introduction impurities, correlation parameters, substitution impurities, B19 structure*

INTRODUCTION

Today, the study of the solubility of impurities introduced into the metal crystal structure is mostly based on the results of research on the production of metals [1–4], alloys [5–7], and their mechanical mixtures [8–10]. Such materials can play the role of catalysts [11–24] for the synthesis of a number of nanostructures (fullerenes [25–28], fullerites [29], endofullerenes [30], nanotubes [31–34] and others [35–39]) in various methods of synthesis [40–46]. All catalysts and related synthesized nanostructures allow to compete with other micro [47–79] and nanofillers [50–58] for modern composites that have more or less a range of applications in various fields: solar panels [59–61], additive technologies [62–65], sorption fields [66–72], biological and medical fields [73–77], as well as in hydrogen energy [78–100].

In the field of hydrogen energy, materials that can serve as hydrogen sorbents [78–100] are of special scientific and practical interest to solve the problem of storing and transporting hydrogen as a power source of the energy “hydrogen cycle”. Both carbon nanostructures [78–82] and metals [83–86] and their alloys [87–100] are being studied to create hydrogen sorbents.

SOLUBILITY, IMPURITIES, IMPLEMENTATION

The solubility of the introduced impurity was studied mainly for alloys with different structures [101, 102], the correlation in the substitution of nodes and internodes – for disordered alloys [103]. In this work, we consider a metal with a

hexagonal structure B19, into the interstices of which insertion atoms are introduced, let's call them C-atoms. The B19 structure has two types of octahedral O_1, O_2 and one type of tetrahedral T internodes. Fig. 1 shows the studied structure in spatial (Fig. 1 *a*) and projection along the C axis (Fig. 1 *b*) images. Black circles show nodes of the first type, legal for A atoms; light circles show nodes of the second type, legal for B atoms; crosses - octapores; points - tetrapores.

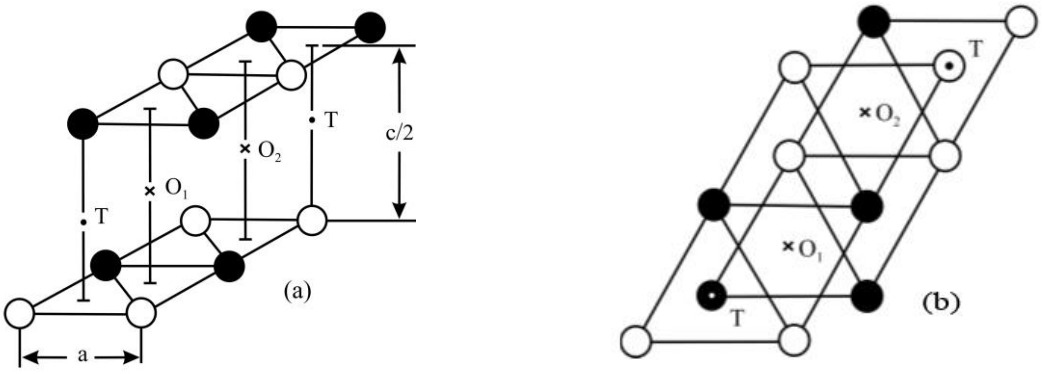

Fig. 1. Image of the hexagonal structure of B19. *a* – spatial image of the B19 structure; *b* – projection image of the B19 structure along the C axis. Black circles (●) show nodes of the first type, legal for A atoms; light circles (o) show nodes of the second type, legal for B atoms; crosses (×) – octapores; dots (•) – tetrapores

To determine the solubility and correlation properties, it is necessary to calculate the free energy of metal F. We use the method of configurations, that is, we take into account all kinds of changes of atoms A for each internode. The configuration is denoted by the index *l*, which determines the number of nearest atoms around the pore. The free energy can be presented in the form specified in formula (1) [102, 103].

$$F=\sum_{l=0}^{6}\left(N_{O_1}^{l}+N_{O_2}^{l}\right)\upsilon_l-\sum_{l=0}^{4}N_T^{l}\upsilon_l'-\kappa\Theta\left[\sum_{l=0}^{6}Q_{O_1}^{l}\ln Q_{O_1}^{l}+\sum_{l=0}^{6}Q_{O_2}^{l}\ln Q_{O_2}^{l}+\sum_{l=0}^{4}Q_T^{l}\ln Q_T^{l}-\right.$$
$$-\sum_{l=0}^{6}N_{O_1}^{l}\ln N_{O_1}^{l}-\sum_{l=0}^{6}N_{O_2}^{l}\ln N_{O_2}^{l}-\sum_{l=0}^{4}N_T^{l}\ln N_T^{l}-\sum_{l=0}^{6}\left(Q_{O_1}^{l}-N_{O_1}^{l}\right)\ln\left(Q_{O_1}^{l}-N_{O_1}^{l}\right)- \quad (1)$$
$$\left.-\sum_{l=0}^{6}\left(Q_{O_2}^{l}-N_{O_2}^{l}\right)\ln\left(Q_{O_2}^{l}-N_{O_2}^{l}\right)-\sum_{l=0}^{4}\left(Q_T^{l}-N_T^{l}\right)\ln\left(Q_T^{l}-N_T^{l}\right)\right],$$

where $N_{O_1}^{l}$, $N_{O_2}^{l}$, N_T^{l} is the number of C atoms in pores O_1, O_2, T ; $Q_{O_1}^{l}$, $Q_{O_2}^{l}$, Q_T^{l} – the number of these pores in the alloy; $\upsilon_1 = l\ \alpha + (6-l)\beta$ $\upsilon_l' = l\alpha' + (4-l)\beta'$ – energies of the C atom in octa- and tetrapores; $\alpha = \upsilon_{AC}$, $\beta = \upsilon_{BC}$ - $\alpha' = \upsilon_{AC}'$, $\beta' = \upsilon_{BC}'$ energy of interaction of the nearest pairs of the specified atoms; *k* – Boltzmann's constant; Θ – absolute temperature.

From the conditions of minimum free energy, we find the numbers

$$N_{O_1}^{l}=\frac{DQ_{O_1}^{l}\exp\frac{\upsilon_l}{\kappa\Theta}}{1+DQ_{O_1}^{l}\exp\frac{\upsilon_l}{\kappa\Theta}};\ N_{O_2}^{l}=\frac{DQ_{O_2}^{l}\exp\frac{\upsilon_l}{\kappa\Theta}}{1+DQ_{O_2}^{l}\exp\frac{\upsilon_l}{\kappa\Theta}};$$
$$N_T^{l}=\frac{DQ_T^{l}\exp\frac{\upsilon_l'}{\kappa\Theta}}{1+DQ_T^{l}\exp\frac{\upsilon_l'}{\kappa\Theta}}, \quad (2)$$

which are connected by an obvious ratio

$$\sum_{l=0}^{6}\left(N_{O_1}^{l}+N_{O_2}^{l}\right)+\sum_{l=0}^{4}N_T^{l}=N_C, \quad (3)$$

where N_C is the number of all C atoms in the alloy. The coefficient *D* included in formulas (2) is a multiplier by which the state function of the system increases when each additional atom appears in it in the process of dissolving impurities. When studying the correlation, if we count N_C = const, the coefficient D is determined from condition (3). Formulas (2) are valid for any numbers of filling of internodes with C atoms.

In the particular case of metal A, when $l = 6$, $\upsilon_l = 6\alpha$, Q_O = N for octapore and $l = 4$, $\upsilon_l' = 4\,\alpha'$, $Q_T = 2N$ for tetrapores (N is the number of alloy nodes), instead of nineteen formulas (2) we have two

$$N_O = N\left(1+\frac{1}{D}\exp\frac{-6\alpha}{\kappa\Theta}\right)^{-1};\quad N_T = 2N\left(1+\frac{1}{D}\exp\frac{-4\alpha'}{\kappa\Theta}\right)^{-1}, \tag{4}$$

summing up them we find the solubility of the component

$$\nu = \frac{N_O+N_T}{3N} = \frac{1}{3}\left[\left(1+\frac{1}{D}\exp\frac{-6\alpha}{\kappa\Theta}\right)^{-1}+2\left(1+\frac{1}{D}\exp\frac{-4\alpha'}{\kappa\Theta}\right)^{-1}\right]. \tag{5}$$

If C atoms are located only in octapores or only in tetrapores, then the solubilities should be determined according to the formulas:

$$\nu_O = \frac{N_O}{N} = \left(1+\frac{1}{D}\exp\frac{-6\alpha}{\kappa\Theta}\right)^{-1};\quad \nu_T = \frac{N_T}{2N} = \left(1+\frac{1}{D}\exp\frac{-4\alpha'}{\kappa\Theta}\right)^{-1}. \tag{6}$$

In the case of low concentrations of the component, these ratios are simplified

$$\nu_O = D\exp\frac{6\alpha}{\kappa\Theta};\quad \nu_T = D\exp\frac{4\alpha'}{\kappa\Theta}, \tag{7}$$

that is, a linear dependence of the natural logarithm of the solubility of the introduced atoms on the inverse temperature is manifested. The dependences of $\ln\nu_O$ and $\ln\nu_T$from $1/\Theta$ (6) are not linear, but monotonic.

If the solubility is described by formula (5), then it is possible to manifest its extreme properties in the temperature dependence at

$$\frac{\alpha}{\alpha'} = -\exp\frac{2(3\alpha-2\alpha')}{\kappa\Theta}; \tag{8}$$

at the same time, the energy parameters α and α' must have different signs. In this case, the distribution of C atoms in the octa- and tetrapores is uneven. It can be estimated from the equations

$$\nu_O+2\nu_T = 3c;\quad \frac{\nu_O(1-\nu_T)}{\nu_T(1-\nu_O)} = \exp\frac{2(3\alpha-2\alpha')}{\kappa\Theta}, \tag{9}$$

where c = Nc/3N. The first is obtained from system (4) by excluding the multiplier *D*, the second is condition (3).

Solving system (9), we find

$$\nu_O = \frac{3c(1-\varepsilon)-2-\varepsilon+\sqrt{\left[3c(1-\varepsilon)-2-\varepsilon\right]^2+12c\varepsilon(1-\varepsilon)}}{2(1-\varepsilon)},$$

$$\nu_T = \frac{3}{2}c-\frac{1}{2}\nu_O, \tag{10}$$

where $\varepsilon = \exp\frac{2(3\alpha-2\alpha')}{\kappa\Theta}$. is marked. When $c = 1$, distribution (10) gives $\nu_O = \nu_T = 1$, that is. we have uniform filling of all internodes regardless of temperature.

At low temperatures, the distribution of atoms is determined by the ratio of energy parameters α and α′. If $3\alpha-2\alpha' > 0$, at absolute zero of temperature we have

$$\nu_O(0) = \begin{cases} 3c\text{at}0 \le c \le \frac{1}{3} \\ 1\text{at}\frac{1}{3} \le c \le 1, \end{cases} \nu_T(0) =$$

$$= \begin{cases} 0 \text{at} 0 \le c \le \frac{1}{3} \\ \frac{3}{2}c - \frac{1}{2} \text{at} \frac{1}{3} \le c \le 1, \end{cases} \quad (11)$$

that is, the introducing atoms first occupy the octapores, in which they have a deeper potential energy minimum, and only when the octapores are occupied do the tetrapores begin to fill. If $3\alpha - 2\alpha' < 0$, then

$$\nu_O(0) = \begin{cases} 0 \text{at} 0 \le c \le \frac{2}{3} \\ 3c - 2 \ \text{at} \frac{2}{3} \le c \le 1, \end{cases} \quad \nu_T(0) =$$

$$= \begin{cases} \frac{3}{2}c \quad \text{at} 0 \le c \le \frac{2}{3} \\ 1 \text{at} \frac{2}{3} \le c \le 1, \end{cases} \quad (12)$$

that is, first of all, C atoms fill the tetrapores. Dependences (11) and (12) are represented by straight lines in Fig. 2. Curved lines in this figure show the dependences of $\nu_O(0)$ and $\nu_T(0)$, constructed according to distribution (10) at the temperatures Θ_1 and Θ_2.

$$\Theta_1 = \frac{4(1{,}5\alpha - \alpha')}{\kappa \ln 10} \quad \text{(a)} \quad \text{and}$$

$$\Theta_2 = -\frac{4(1{,}5\alpha - \alpha')}{\kappa \ln 10} \quad \text{(b)}$$

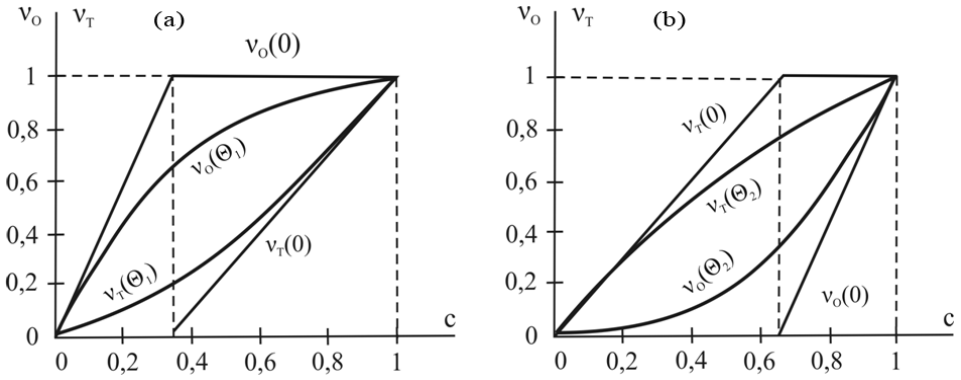

Fig. 2. Graphic representation of dependences (11), (12), and $\nu_O(0)$ and $\nu_T(0)$ according to distribution (10) at the temperatures Θ_1 (*a*) and Θ_2 (*b*)

It is necessary to consider the second special case - a binary alloy with a low concentration of the introduction impurity. In this case, relation (2) is simplified:

$$N_{O_1}^l = DQ_{O_1}^l \exp\frac{\upsilon_l}{\kappa\Theta}; \ N_{O_2}^l = DQ_{O_2}^l \exp\frac{\upsilon_l}{\kappa\Theta}; \ \ N_T^l = DQ_T^l \exp\frac{\upsilon_l'}{\kappa\Theta}, \quad (13)$$

and $Q_{O_1}^l$, $Q_{O_2}^l$, Q_T^l numbers are determined by the configuration of A atoms around voids

$$Q_{O_1}^l = \frac{1}{2} N \frac{4!}{i!(4-i)!} p_A^{(1)i} p_B^{(1)(4-i)} \cdot \frac{2!}{j!(2-j)!} p_A^{(2)j} p_B^{(2)(2-j)}$$

$$Q_{O_2}^l = \frac{1}{2} N \frac{2!}{i!(2-i)!} p_A^{(1)i} p_B^{(1)(2-i)} \cdot \frac{4!}{j(4-j)!} p_A^{(2)j} p_B^{(2)(4-j)}$$

$$Q_T^l = 2N \frac{2!}{i!(2-i)!} p_A^{(1)i} p_B^{(1)(2-i)} \cdot \frac{2!}{j!(2-j)!} p_A^{(2)j} p_B^{(2)(2-j)} \quad (14)$$

Here $l = i + j$, where i and j are the numbers of A atoms around the internode, respectively, on nodes of the first and second type, and $p_A^{(1)}$, $p_A^{(2)}$, $p_B^{(1)}$, $p_B^{(2)}$ are the probabilities of replacing nodes 1, 2 by atoms A, B, which depend on the composition *a,* b of the binary alloy and the degree of long-range order η according to the formulas [104]:

$$p_A^{(1)} = a + \frac{1}{2}\eta; \ p_A^{(2)} = a - \frac{1}{2}\eta; \ p_B^{(1)} = b - \frac{1}{2}\eta;$$

$$p_B^{(2)} = b + \frac{1}{2}\eta. \quad (15)$$

Summing up for all configurations of the quantity (13) taking into account (14), we obtain the numbers of C atoms in the pores O_1, O_2, T:

$$N_C^{O_1}=\frac{1}{2}NDK_1^4K_2^2\ ;\ N_C^{O_2}=\frac{1}{2}NDK_1^2K_2^4\ ,\ N_C^{(T)}=2NDK_1'^2K_2'^2 \tag{16}$$

where

$$\begin{aligned}
&\mathrm{K}_1=\mathrm{p}_\mathrm{A}^{(1)}\exp\frac{\alpha}{\kappa\Theta}+\mathrm{p}_\mathrm{B}^{(1)}\exp\frac{\beta}{\kappa\Theta}\ ;\\
&\mathrm{K}_2=\mathrm{p}_\mathrm{A}^{(2)}\exp\frac{\alpha}{\kappa\Theta}+\mathrm{p}_\mathrm{B}^{(2)}\exp\frac{\beta}{\kappa\Theta}\ ;\\
&\mathrm{K}_1'=\mathrm{p}_\mathrm{A}^{(2)}\exp\frac{\alpha'}{\kappa\Theta}+\mathrm{p}_\mathrm{B}^{(1)}\exp\frac{\beta'}{\kappa\Theta};\\
&\mathrm{K}_2'=\mathrm{p}_\mathrm{A}^{(2)}\exp\frac{\alpha'}{\kappa\Theta}+\mathrm{p}_\mathrm{B}^{(2)}\exp\frac{\beta'}{\kappa\Theta}\ .
\end{aligned} \tag{17}$$

The solubility of impurities, which is determined by the concentration of C atoms for each type of internodes, is obtained from (16)

$$v_O=\frac{N_C^{(O_1)}+N_C^{(O_2)}}{N}=\frac{1}{2}DK_1^2K_2^2\left(K_1^2+K_2^2\right),$$

$$v_T=\frac{N_C^{(T)}}{2N}=DK_1'^2K_2'^2. \tag{18}$$

These formulas together with (17) and (15) determine the dependence of solubility on alloy composition, temperature, and order parameters. The first dependence for a disordered alloy ($\eta = 0$) turns out to be monotonic, the second at $\eta = 0$ can be extreme, if

$$\frac{\alpha}{\beta}=-\frac{b}{a}\exp\frac{\beta-\alpha}{\kappa\Theta}$$

for the octa pores and

$$\frac{\alpha'}{\beta'}=-\frac{b}{a}\exp\frac{\beta'-\alpha'}{\kappa\Theta}$$

for tetrapores (in this case, the energy parameters α, β and α', β' must have different signs). The influence of atomic order on solubility is convenient to find out for relative values (Fig. 3).

$$f_O=v_O/\left(v_O\right)_{\eta=0}=\left(1-\chi_1^2\right)\left(1-\chi_1^4\right),$$

$$f_T=v_T/\left(v_T\right)_{\eta=0}=\left(1-\chi_2^2\right)^2, \tag{19}$$

where

$$\chi_1=\frac{1}{2}\eta\frac{\exp\frac{\alpha}{\kappa\Theta}-\exp\frac{\beta}{\kappa\Theta}}{a\exp\frac{\alpha}{\kappa\Theta}+b\exp\frac{\beta}{\kappa\Theta}};$$

$$\chi_2=\frac{1}{2}\eta\frac{\exp\frac{\alpha'}{\kappa\Theta}-\exp\frac{\beta'}{\kappa\Theta}}{a\exp\frac{\alpha'}{\kappa\Theta}+b\exp\frac{\beta'}{\kappa\Theta}};$$

$$-1\le\chi_1,\ \ \chi_2<1. \tag{20}$$

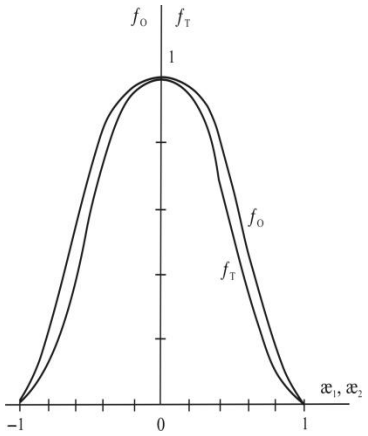

Fig. 3. Influence of atomic order on solubility

The nature of the dependence of the values f_O, f_T on η is the same. Ordering reduces solubility, for octapores this reduction is somewhat weaker.

In the case of distribution of the introduction impurity simultaneously on all internodes, the solubility is determined by the formula

$$v=\frac{N_C^{(O_1)}+N_C^{(O_2)}+N_C^{(T)}}{3N}=$$

$$=\frac{1}{6}D\left[K_1^2K_2^2\left(K_1^2+K_2^2\right)+4K_1'^2K_2'^2\right]. \tag{21}$$

The dependence of solubility on the composition at $\eta = 0$ can be extreme if the energies α and β or α' and β' are of different signs.

The nature of the dependence of ν on η is the same as for the values ν_O and ν_T.

Let's find the correlation parameters in the substitution of nodes and internodes, counting N_C = const. From condition (3) taking into account (13), we find the coefficient *D*

$$D = 6c[K_1^2 K_2^2 (K_1^2 + K_2^2) + 4K_1'^2 K_2'^2]^{-1}. \qquad (22)$$

Summing up the values of $N_{O_1}^l$, $N_{O_2}^l$, N_T^l (13) over *i* or *j*, we will find the number of C atoms in the specified pores with the corresponding *i-th* or *j-th* configuration of A atoms, on the nodes of one type closest to the internode, with any filling of nodes of another type:

$$N_{O_1}^i = \sum_{j=0}^{2} N_{O_1}^l = \frac{1}{2} DNK_2^2 \frac{4!}{i!(4-i)!} p_A^{(l)i} p_B^{(l)(4-i)} \exp\frac{i\alpha + (4-i)\beta}{\kappa\Theta};$$

$$N_{O_1}^j = \sum_{i=0}^{4} N_{O_1}^l = \frac{1}{2} DNK_1^4 \frac{2!}{j!(2-j)!} p_A^{(2)j} p_B^{(2)(2-j)} \exp\frac{j\alpha + (2-j)\beta}{\kappa\Theta};$$

$$N_{O_2}^i = \sum_{j=0}^{4} N_{O_2}^l = \frac{1}{2} DNK_2^4 \frac{2!}{i!(2-i)!} p_A^{(1)j} p_B^{(1)(2-i)} \exp\frac{i\alpha + (2-i)\beta}{\kappa\Theta}; \qquad (23)$$

$$N_{O_2}^j = \sum_{i=0}^{2} N_{O_2}^l = \frac{1}{2} DNK_1^2 \frac{4!}{j!(4-j)!} p_A^{(2)j} p_B^{(2)(4-j)} \exp\frac{j\alpha + (4-j)\beta}{\kappa\Theta};$$

$$N_T^i = \sum_{j=0}^{2} N_T^l = 2DNK_2'^2 \frac{2!}{i!(2-j)!} p_A^{(1)i} p_B^{(1)(2-i)} \exp\frac{i\alpha' + (2-i)\beta'}{\kappa\Theta};$$

$$N_T^j = \sum_{i=0}^{2} N_T^l = 2DNK_1'^2 \frac{2!}{j!(2-j)!} p_A^{(2)j} p_B^{(2)(2-j)} \exp\frac{j\alpha' + (2-j)\beta'}{\kappa\Theta}.$$

The posteriori and a priori probabilities of replacement of the nearest pairs of nodes and pores by atoms A, C are equal, respectively

$$p_{AC}^{(1O_1)} = \frac{1}{2N} \sum_{i=0}^{4} iN_{O_1}^i = DK_1^3 K_2^2 p_A^{(1)} \exp\frac{\alpha}{\kappa\Theta}; \quad p_{AC}^{(1O_1)^0} = 2p_A^{(1)} N_C^{(O_1)} / N = DK_1^4 K_2^2 p_A^{(1)};$$

$$p_{AC}^{(2O_1)} = \frac{1}{N} \sum_{j=0}^{2} jN_{O_1}^j = DK_1^4 K_2 p_A^{(2)} \exp\frac{\alpha}{\kappa\Theta}; \quad p_{AC}^{(2O_1)^0} = 2p_A^{(2)} N_C^{(O_1)} / N = DK_1^4 K_2^2 p_A^{(2)};$$

$$p_{AC}^{(1O_2)} = \frac{1}{N} \sum_{i=0}^{2} iN_{O_2}^i = DK_1 K_2^4 p_A^{(1)} \exp\frac{\alpha}{\kappa\Theta}; \quad p_{AC}^{(1O_2)^0} = 2p_A^{(1)} N_C^{(O_2)} / N = DK_1^2 K_2^4 p_A^{(1)}; \qquad (24)$$

$$p_{AC}^{(2O_2)} = \frac{1}{2N} \sum_{j=0}^{4} jN_{O_2}^j = DK_1^2 K_2^3 p_A^{(2)} \exp\frac{\alpha}{\kappa\Theta}; \quad p_{AC}^{(2O_2)^0} = 2p_A^{(2)} N_C^{(O_2)} / N = DK_1^2 K_2^4 p_A^{(2)};$$

$$p_{AC}^{(1T)} = \frac{1}{4N} \sum_{i=0}^{2} iN_T^i = DK_1' K_2'^2 p_A^{(1)} \exp\frac{\alpha'}{\kappa\Theta}; \quad p_{AC}^{(1T)^0} = \frac{1}{2} p_A^{(1)} N_C^{(T)} / N = DK_1'^2 K_2'^2 p_A^{(1)};$$

$$p_{AC}^{(2T)} = \frac{1}{4N} \sum_{j=0}^{2} jN_T^j = DK_1'^2 K_2' p_A^{(2)} \exp\frac{\alpha'}{\kappa\Theta}; \quad p_{AC}^{(2T)^0} = \frac{1}{2} p_A^{(2)} N_C^{(T)} / N = DK_1'^2 K_2'^2 p_A^{(2)}.$$

The differences in these possibilities determine the correlation parameters. Similarly, correlation parameters can be found for pairs of B, C atoms. Using calculations, we find

$$\varepsilon^{(1O_1)} = \varepsilon_{AC}^{(1O_1)} = -\varepsilon_{BC}^{(1O_1)} = DK_1^3 K_2^2 p_A^{(1)} p_B^{(1)} (\exp\frac{\alpha}{\kappa\Theta} - \exp\frac{\beta}{\kappa\Theta});$$

$$\varepsilon^{(2O_1)} = \varepsilon_{AC}^{(2O_1)} = -\varepsilon_{BC}^{(2O_1)} = DK_1^4 K_2 p_A^{(2)} p_B^{(2)} (\exp\frac{\alpha}{\kappa\Theta} - \exp\frac{\beta}{\kappa\Theta});$$

$$\varepsilon^{(1O_2)} = \varepsilon_{AC}^{(1O_2)} = -\varepsilon_{BC}^{(1O_2)} = DK_1 K_2^4 p_A^{(1)} p_B^{(1)} (\exp\frac{\alpha}{\kappa\Theta} - \exp\frac{\beta}{\kappa\Theta});$$

$$\varepsilon^{(2O_2)} = \varepsilon_{AC}^{(2O_2)} = -\varepsilon_{BC}^{(2O_2)} = DK_1^2 K_2^3 p_A^{(2)} p_B^{(2)} (\exp\frac{\alpha}{\kappa\Theta} - \exp\frac{\beta}{\kappa\Theta});$$

$$\varepsilon^{(1T)} = \varepsilon_{AC}^{(1T)} = -\varepsilon_{BC}^{(1T)} = DK_1' K_2'^2 p_A^{(1)} p_B^{(1)} (\exp\frac{\alpha'}{\kappa\Theta} - \exp\frac{\beta'}{\kappa\Theta});$$

$$\varepsilon^{(2T)} = \varepsilon_{AC}^{(2T)} = -\varepsilon_{BC}^{(2T)} = DK_1'^2 K_2' p_A^{(2)} p_B^{(2)} (\exp\frac{\alpha'}{\kappa\Theta} - \exp\frac{\beta'}{\kappa\Theta}). \quad (25)$$

The obtained formulas, taking into account (22), (17) and (15), determine the dependence of the correlation parameters on the composition of the alloy, temperature, and the degree of long-range order, the knowledge of which can allow determining the formation of short-range ordering or stratification of atoms in the alloy. The correlation parameters for octapore and tetrapore can be of different signs, for example, when $\alpha > \beta$ and $\alpha' < \beta'$. This means that C atoms will primarily concentrate in the octahedral interstices. For a disordered alloy

($\eta = 0$, $K = K_1 = K_2 =$

$$= a\exp\frac{\alpha}{\kappa\Theta} + b\exp\frac{\beta}{\kappa\Theta},$$

$$K' = K_1' = K_2' = a\exp\frac{\alpha'}{\kappa\Theta} + b\exp\frac{\beta'}{\kappa\Theta})$$

only two correlation parameters are preserved for pores O and T:

$$\varepsilon^{(O)} = 3abcK^5 (\exp\frac{\alpha}{\kappa\Theta} - \exp\frac{\beta}{\kappa\Theta}) / (K^6 + 2K'^4);$$

$$\varepsilon^{(T)} = 3abcK'^3 (\exp\frac{\alpha'}{\kappa\Theta} - \exp\frac{\beta'}{\kappa\Theta}) / (K^6 + 2K'^4). \quad (26)$$

The dependence of the $\varepsilon^{(0)}$ and $\varepsilon^{(T)}$ values on the composition is extreme and asymmetric. The maximum of this dependence is manifested in the composition

$$a_* = (\exp\frac{\alpha - \beta}{2\kappa\Theta} + 1)^{-1}.$$

For $\varepsilon^{(O)}$ and at $a_* = (\exp\frac{\alpha' - \beta'}{\kappa\Theta} + 1)^{-1}$ for $\varepsilon^{(T)}$. As the temperature increases, the asymmetry of the concentration dependence decreases, and at very high temperatures the value of a_* is close to the stoichiometric composition of ($a_* \approx 1/2$). At high temperatures, formulas (26) are simplified

$$\varepsilon^{(O)} = abc\frac{\alpha - \beta}{\kappa\Theta}; \quad \varepsilon^{(T)} = abc\frac{\alpha' - \beta'}{\kappa\Theta}. \quad (27)$$

Finally, we will write down the formulas for the correlation parameters in the case of distribution of atoms only in octapores or only in tetrapores. In the first case $c = Nc/N$, $D = 2c[K_1 K_2 (K_1^2 + K_2^2)]^{-1}$ and

$$\varepsilon^{(1O_1)} = 2cp_A^{(1)} p_B^{(1)} (\exp\frac{\alpha}{\kappa\Theta} - \exp\frac{\beta}{\kappa\Theta}) K_1 / (K_1^2 + K_2^2);$$

$$\varepsilon^{(2O_1)} = 2cp_A^{(2)} p_B^{(2)} (\exp\frac{\alpha}{\kappa\Theta} - \exp\frac{\beta}{\kappa\Theta}) K_1^2 / K_2 (K_1^2 + K_2^2);$$

$$\varepsilon^{(1O_2)} = 2cp_A^{(1)}p_B^{(1)}(\exp\frac{\alpha}{\kappa\Theta} - \exp\frac{\beta}{\kappa\Theta})K_2^2 / K_1(K_1^2 + K_2^2);$$
$$\varepsilon^{(2O_2)} = 2cp_A^{(2)}p_B^{(2)}(\exp\frac{\alpha}{\kappa\Theta} - \exp\frac{\beta}{\kappa\Theta})K_2 / (K_1^2 + K_2^2); \quad (28)$$

in the second $c = Nc/2N$, $D = c(K_1' + K_2')^{-2}$ and

$$\varepsilon^{(1T)} = cp_A^{(1)}p_B^{(1)}(\exp\frac{\alpha'}{\kappa\Theta} - \exp\frac{\beta'}{\kappa\Theta}) / K_1',$$
$$\varepsilon^{(2T)} = cp_A^{(2)}p_B^{(2)}(\exp\frac{\alpha'}{\kappa\Theta} - \exp\frac{\beta'}{\kappa\Theta}) / K_2'. \quad (29)$$

CONCLUSIONS

Knowing the correlation parameters (25) or (29) and (28) allows one to estimate many physical characteristics of alloys. If the correlation parameters are known from experiments, the obtained formulas allow one determining the energy parameters of alloys, which has a high scientific value.

Атоми впровадження у кристалічній гексагональній структурі

З.А. Матисіна, Ан.Д. Золотаренко, Ол.Д. Золотаренко, Т.В. Мироненко, Д.В. Щур, О.П. Рудакова, М.В. Чимбай, О.Д. Золотаренко, І.В. Загорулько, О.О. Гаврилюк

Інститут проблем матеріалознавства ім. І.М. Францевича Національної академії наук України
вул. Кржижанівського, 3, Київ, 03142, Україна, a.d.zolotarenko@gmail.com
Інститут хімії поверхні ім. О.О. Чуйка Національної академії наук України
вул. Генерала Наумова, 17, Київ, 03164, Україна, o.d.zolotarenko@gmail.com
Інститут металофізики ім. Г.В. Курдюмова Національної академії наук України
бульв. Академіка Вернадського, 36, Київ, 03142, Україна
Інститут прикладної фізики Національної академії наук України
вул. Петропавлівська, 58, Суми, 40000, Україна

В рамках роботи розглянуто гексагональну структуру металів типу B19 як сорбентів водню. Розглядаються кристалічні ґратки, де в міжвузлі металу впроваджуються атоми домішок (водень). Для цього у роботі наведено зображення самої структури B19. В роботі вивчено розчинність водню в кристалічній структурі металів типу B19, використовуючи метод конфігурацій, а також знайдено в заміщенні вузлів і міжвузлів залежність від складу сплаву та температури. Також розглянуто ступінь далекого порядку у вузлах та визначено параметри кореляції у заміщенні. Наведено графічний вигляд впливу атомного порядку на розчинність домішок. Розрахункові дані, які отримані у роботі, збігаються з експериментальними даними інших досліджень, а отримані формули розрахунків дозволяють визначити енергетичні параметри сплавів, що мають певну наукову цінність. Запропонована система враховує лише атомну взаємодію та абсорбцію (розчинення), дифузію атомів впровадження в об'єм кристалічної структури, тому можна прогнозувати введення лише атома водню). Таким чином, отримані в роботі результати щодо параметрів кореляції при розподілі атомів лише в октапорах або лише в тетрапорах дозволяють глибше вивчати фізичні характеристики сплавів типу B19 і зрозуміти процеси сорбції водню робочими тілами для накопичувачів водню.

***Ключові слова**: водень, метал, сплави, розчинність, введення домішок, кореляційні параметри, домішки заміщення, структура B19*

REFERENCES

1. Nastasiienko N., Palianytsia B., Kartel M., Larsson M., Kulik T. Thermal transformation of caffeic acid on the nanoceria surface studied by temperature programmed desorption mass-spectrometry, thermogravimetric analysis and ft–ir spectroscopy. *Colloids and Interfaces*. 2019. **3**(1): 34.
2. Abdullin K.A., Gabdullin M.T., Gritsenko L.V., Ismailov D.V., Kalkozova Z.K., Kumekov S.E., Mukash Z.O., Sazonov A.Y., Terukov E.I. Electrical, optical, and photoluminescence properties of ZnO films subjected to thermal annealing and treatment in hydrogen plasma. *Semiconductors*. 2016. **50**(8): 1010.
3. Mostovshchikov A.V., Ilyin A.P., Zabrodina I.K., Root L.O., Ismailov D.V. Measuring the changes in copper nanopowder conductivity during heating as a method for diagnosing its thermal stability. *Key Eng. Mater*. 2018. **769**: 146.
4. Baglyuk G.A., Ivasyshyn O.M., Stasyuk O.O., Savvakin D.G. Sintered metals and alloys: The effect of charge component composition on the structure and properties of titanium matrix sintered composites with high-modulus compounds. *Powder Metall. Met. Ceram*. 2017. **56**(1–2): 59.
5. Baglyuk G.A., Sosnovskii L.A., Volfman V.I. Effect of carbon content on the properties of sintered steels doped with manganese and copper. *Powder Metall. Met. Ceram*. 2011. **50**(3–4): 189.
6. Baglyuk G.A., Tolochin A.I., Tolochina A.V., Yakovenko R.V., Gripachevckii A.N., Golovkova M.E. Effect of Process Conditions on the Structure and Properties of the Hot-Forged Fe_3Al Intermetallic Alloy. *Powder Metall. Met. Ceram.* 2016. **55**(5–6): 297.
7. Baglyuk G.A., Poznyak L.A. Sintered wear-resistant iron-based materials. I. Materials fabricated by sintering and impregnation. *Powder Metallurgy*. 2001. **(1–2)**: 44.
8. Sizonenko O.N., Baglyuk G.A., Taftai E.I., Zaichenko A.D., Lipyan E.V., Torpakov A.S., Zhdanov A.A., Pristash N.S. Dispersion and carburization of titanium powders by electric discharge. *Powder Metall. Met. Ceram*. 2013. **52**(5–6): 247.
9. Ivashchenko V.I., Veprek S., Turchi P.E.A., Shevchenko V.I., Leszczynski J., Gorb L., Hill F. First-principles molecular dynamics investigation of thermal and mechanical stability of the TiN(001)/AlN and ZrN(001)/AlN heterostructures. *Thin Solid Films*. 2014. **564**: 284.
10. Baglyuk G.A., Napara-Volgina S.G., Vol'Fman V.I., Mamonova A.A., Pyatachuk S.G. Thermal synthesis of Fe-B 4C powder master alloys. *Powder Metall. Met. Ceram*. 2009. **48**(7–8): 381.
11. Havryliuk O.O., Semchuk O.Y. Formation of periodic structures on the solid surface under laser irradiation. *Ukr. J. Phys*. 2017. **62**(1): 20.
12. Ivashchenko V.I., Shevchenko V.I. Effects of short-range disorder upon electronic properties of a-SiC alloys. *Appl. Surf. Sci*. 2001. **184**(1–4): 137.
13. Biliuk A.A., Semchuk O.Y., Havryliuk O.O. Width of the surface plasmon resonance line in spherical metal nanoparticles. *Semicond. Phys. Quantum Electron. Optoelectron*. 2020. **23**(3): 308.
14. Baglyuk G.A., Poznyak L.A. The sintering of powder metallurgy high-speed steel with activating additions. *Powder Metall. Met. Ceram*. 2002. **41**(7–8): 366.
15. Ilyin A.P., Mostovshchikov A.V., Root L.O., Zmanovskiy S.V., Ismailov D.V., Ruzieva G.U. Effect of beta-radiation exposure on the parameters of aluminum micropowders activity. *Bulletin of the Tomsk Polytechnic University, Geo Assets Engineering*. 2019. **330**(8): 87.
16. Ivashchenko V.I., Turchi P.E.A., Shevchenko V.I. Phase transformation B1 to B2 in TiC, TiN, ZrC and ZrN under pressure. *Condens. Matter Phys.* 2013. **16**(3): 33602.
17. Onoprienko A.A., Ivashchenko V.I., Dub S.N., Khyzhun O.Y., Timofeeva I.I. Microstructure and mechanical properties of hard Ti-Si-C-N films deposited by dc magnetron sputtering of multicomponent Ti/C/Si target. *Surf. Coat. Technol*. 2011. **205**(21–22): 5068.
18. Khomenko E.V., Baglyuk G.A., Minakova R.V. Effect of deformation processing on the properties of Cu-50 % Cr composite. *Powder Metall. Met. Ceram*. 2009. **48**(3-4): 211.
19. Kozak A.O., Ivashchenko V.I., Porada O.K., Ivashchenko L.A., Tomila T.V., Manjara V.S., Klishevych G.V. Structural, optoelectronic and mechanical properties of PECVD Si-C-N films: An effect of substrate bias. *Mater. Sci. Semicond. Process*. 2018. **88**: 65.
20. Semchuk O.Y., Biliuk A.A., Havryliuk O.O. The Kinetic Theory of the Width of Surface Plasmon Resonance Line in Metal Nanoparticles. *Springer Proceedings in Physics*. 2021. **264**: 3.
21. Ivashchenko V.I., Turchi P.E.A., Shevchenko V.I., Olifan E.I. First-principles study of phase stability of stoichiometric vanadium nitrides. *Phys. Rev. B*. 2011. **84**(17): 174108.
22. Baglyuk G.A., Terekhov V.N., Ternovoi Y.F. Structure and properties of powder austenitic die steels. *Powder Metall. Met. Ceram*. 2006. **45**(7–8): 317.

23. Tolochyn O.I., Baglyuk G.A., Tolochyna O.V., Evych Y.I., Podrezov Y.M., Molchanovska H.M. Structure and Physicomechanical Properties of the Fe_3Al Intermetallic Compound Obtained by Impact Hot Compaction. *Mater. Sci.* 2021. **56**(4): 499.
24. Ivashchenko V.I., Vepřek S. First-principles molecular dynamics study of the thermal stability of the BN, AlN, SiC and SiN interfacial layers in TiN-based heterostructures: Comparison with experiments. *Thin Solid Films.* 2013. **545**: 391.
25. Zaginaichenko S.Y., Lysenko E.A., Golovchenko T.N., Javadov N.F. The forming peculiarities of C_{60} molecule. *NATO Science for Peace and Security Series C: Environmental Security*. 2008. **Part F2**: 53.
26. Zolotarenko Ol.D., Rudakova E.P., Akhanova N.Yu., Zolotarenko An.D., Shchur D.V., Matysina Z.A., Gabdullin M.T., Ualkhanova M., Gavrylyuk N.A., Zolotarenko A.D., Chymbai M.V., Zagorulko I.V. Comparative Analysis of Products of the Fullerenes' and Carbon-Nanostructures' Synthesis Using the SIGE and FGDG-7 Grades of Graphite. *Nanosystems, Nanomaterials, Nanotechnologies*. 2022. **20**(3): 725.
27. Gun'ko V.M., Turov V.V., Zarko V.I., Prykhod'ko G.P., KrupskaT.V., Golovan A.P., Skubiszewska-Zięba J., Charmas B., Kartel M.T. Unusual interfacial phenomena at a surface of fullerite and carbon nanotubes. *Chem. Phys*. 2015. **459**: 172.
28. Nishchenko M.M., Likhtorovich S.P., Dubovoy A.G., Rashevskaya T.A. Positron annihilation in C_{60} fullerites and fullerene-like nanovoids. *Carbon*. 2003. **41**(7): 1381.
29. Lad'yanov V.I., Nikonova R.M., Larionova N.S., Aksenova V.V., Mukhgalin V.V., Rud' A.D. Deformation-induced changes in the structure of fullerites $C_{60/70}$ during their mechanical activation. *Phys. Solid State*. 2013. **55**(6): 1319.
30. Matysina Z.A., Zolotarenko Ol.D., Rudakova O.P., Akhanova N.Y., Pomytkin A.P., Zolotarenko An.D., Shchur D.V., Gabdullin M.T., Ualkhanova M., Gavrylyuk N.A., Zolotarenko A.D., Chymbai M.V., Zagorulko I.V. Iron in Endometallofullerenes. *Prog. Phys. Met.* 2022. **23**(3): 510.
31. Sementsov Yu.I., Cherniuk O.A., Zhuravskyi S.V., Bo W., Voitko K.V., Bakalinska O.M., Kartel M.T. Synthesis and catalytic properties of nitrogen-containing carbon nanotubes. *Him. Fiz. Tehnol. Poverhni*. 2021. **12**(2): 135.
32. Ushakova L.M., Ivanenko K.I., Sigareva N.V., Terets M.I., Kartel M.T., Sementsov Yu.I. Influence of nanofiller on the structure and properties of macromolecular compounds. *Phys. Chem. Solid State.* 2022. **23**(2): 394.
33. Sementsov Y., Prikhod'ko G., Kartel M., Tsebrenko M., Aleksyeyeva T., Ulyanchychi N. Carbon nanotubes filled composite materials. *NATO Science for Peace and Security Series C: Environmental Security*. 2011. **2**: 183.
34. Harea E., Stoček R., Storozhuk L., Sementsov Y., Kartel N. Study of tribological properties of natural rubber containing carbon nanotubes and carbon black as hybrid fillers. *Appl. Nanosci*. 2019. **9**(5): 899.
35. Schur D.V., Dubovoy A.G., Zaginaichenko S.Yu., Adejev V.M., Kotko A.V., Bogolepov V.A., Savenko A.F., Zolotarenko A.D., Firstov S.A., Skorokhod V.V. Synthesis of carbon nanostructures in gaseous and liquid medium. *NATO Security through Science Series A: Chemistry and Biology*. 2007: 199.
36. Zaginaichenko S.Y., Matysina Z.A. The peculiarities of carbon interaction with catalysts during the synthesis of carbon nanomaterials. *Carbon*. 2003. **41**(7): 1349.
37. Rud A.D., Kiryan I.M. Quantitative analysis of the local atomic structure in disordered carbon. *J. Non-Cryst. Solids*. 2014. **386**: 1.
38. Matvienko Y., Rud A., Polishchuk S., ZagorodniyY., Rud N., Trachevski V. Effect of graphite additives on solid-state reactions in eutectic Al–Cu powder mixtures during high-energy ball milling. *Appl. Nanosci*. 2020. **10**(8): 2803.
39. Kartel M.T., Voitko K.V., Grebelna Y.V., Zhuravskyi S.V., Ivanenko K.O., Kulyk T.V., Makhno S.M., Sementsov Y.I. Changes in the structure and properties of graphene oxide surfaces during reduction and modification. *Him. Fiz. Tehnol. Poverhni*. 2022. **13**(2): 179.
40. Boguslavskii L.Z., Rud' A.D., Kir'yan I.M., Nazarova N.S., Vinnichenko D.V. Properties of carbon nanomaterials produced from gaseous raw materials using high-frequency electrodischarge processing. *Surf. Eng. Appl. Electrochem*. 2015. **51**(2): 105.
41. Matysina Z.A. , Zolotarenko Ol.D. , Ualkhanova M., Rudakova O.P., Akhanova N.Y., Zolotarenko An.D., Shchur D.V., Gabdullin M.T., Gavrylyuk N.A., Zolotarenko O.D., Chymbai M.V., Zagorulko I.V. Electric Arc Methods to Synthesize Carbon Nanostructures. *Prog. Phys. Met*. 2022. **23**(3): 528.
42. Yakymchuk O.M., Perepelytsina O.M., Rud A.D., Kirian I.M., Sydorenko M.V. Impact of carbon nanomaterials on the formation of multicellular spheroids by tumor cells. *Phys. Status Solidi A.* 2014. **211**(12): 2778.
43. Kartel N.T., Gerasimenko N.V., Tsyba N.N., Nikolaichuk A.D., Kovtun G.A. Synthesis and study of carbon sorbent prepared from polyethylene terephthalate. *Russ. J. Appl. Chem.* 2001. **74**(10): 1765.

44. Zolotarenko Ol.D, Ualkhanova M.N., Rudakova E.P., Akhanova N.Y., Zolotarenko An.D., Shchur D.V., Gabdullin M.T., Gavrylyuk N.A., Zolotarenko A.D., Chymbai M.V., Zagorulko I.V., Havryliuk O.O. Advantage sand disadvantages of electric arc methods for thes ynthesis of carbon nanostructures. *Him. Fiz. Tehnol. Poverhni*. 2022. **13**(2): 209. [in Ukrainian].
45. Oreshkin V.I., Chaikovskii S.A., Labetskaya N.A., Ivanov Y.F., Khishchenko K.V., Levashov P.R., Kuskova N.I., Rud' A.D. Phase transformations of carbon under extreme energy action. *Tech. Phys*. 2012. **57**(2): 198.
46. Rud A.D., Lakhnik A.M., Mikhailova S.S., Karban O.V., Surnin D.V., Gilmutdinov F.Z. Structure of Mg-C nanocomposites produced by mechano-chemical synthesis. *J. Alloys Compd*. 2011. **509**(SUPPL. 2): S592.
47. Karachevtseva L., Kartel M., Kladko V., Gudymenko O., Bo W., Bratus V., Lytvynenko O., Onyshchenko V., Stronska O. Functionalization of 2D macroporous silicon under the high-pressure oxidation. *Appl. Surf. Sci*. 2018. **434**: 142.
48. Kozak A.O., Porada O.K., Ivashchenko V.I., Ivashchenko L.A., Scrynskyy P.L., Tomila T.V., Manzhara V.S. Comparative investigation of Si-C-N Films prepared by plasma enhanced chemical vapour deposition and magnetron sputtering. *Appl. Surf. Sci*. 2017. **425**: 646.
49. Ivashchenko V.I., Turchi P.E.A., Shevchenko V.I. Simulations of indentation-induced phase transformations in crystalline and amorphous silicon. *Phys. Rev. B.* 2008. **78**(3): 035205.
50. Krupskaya T.V., Turov V.V., Barvinchenko V.M., Filatova K.O., Suvorova L.A., Iraci G., Kartel M.T. Influence of the "wetting–drying" compaction on the adsorptive characteristics of nanosilica A-300. *Adsorpt. Sci. Technol*. 2018. **36**(1–2): 300.
51. Gun'ko V.M., Turov V.V., Pakhlov E.M., Matkovsky A.K., Krupska T.V., Kartel M.T., Charmas B. Blends of amorphous/crystalline nanoalumina and hydrophobic amorphous nanosilica. *J. Non-Cryst. Solids*. 2018. **500**: 351.
52. Barany S., Kartel' N., Meszaros R. Electrokinetic potential of multilayer carbon nanotubes in aqueous solutions of electrolytes and surfactants. *Colloid J.* 2014. **76**(5): 509.
53. Gun'ko V.M., Turov V.V., Krupska T.V., Protsak I.S., Borysenko M.V., Pakhlov E.M. Polymethylsiloxane alone and in composition with nanosilica under various conditions. *J. Colloid Interface Sci*. 2019. **541**: 213.
54. Biliuk A.A., Semchuk O.Y., Havryliuk O.O. Kinetic theory of absorption of ultrashort laser pulses by ensembles of metallic nanoparticles under conditions of surface plasmon resonance. *Him. Fiz. Tehnol. Poverhni*. 2022. **13**(2): 556.
55. Gun'ko V.M., Turov V.V., Krupska, T.V., Pakhlov E.M. Behavior of water and methane bound to hydrophilic and hydrophobic nanosilicas and their mixture. *Chem. Phys. Lett.* 2017. **690**: 25.
56. Gun'ko V.M., Turov V.V., Protsak I., Krupska T.V., Pakhlov E.M., Zhang D. Interfacial phenomena in composites with nanostructured succinic acid bound to hydrophilic and hydrophobic nanosilicas. *Colloid Interface Sci. Commun*. 2020. **35**: 100251.
57. Protsak I., Gun'ko V.M., Turov V.V., Krupska T.V., Pakhlov E.M., Zhang D., Dong W., Le Z. Nanostructured polymethylsiloxane/fumed silica blends. *Mater*. 2019. **12**(15): 2409.
58. Turov V.V., Gun'ko V.M., Krupska T.V., Borysenko M.V., Kartel M.T. Interfacial behavior of polar and nonpolar frozen/unfrozen liquids interacting with hydrophilic and hydrophobic nanosilicas alone and in blends. *J. Colloid Interface Sci*. 2021. **588**: 70.
59. Pylypova O., Havryliuk O., Antonin S., Evtukh A., Skryshevsky V., Ivanov I., Shmahlii S. Influence of nanostructure geometry on light trapping in solar cells. *Appl. Nanosci.* 2022. **12**(3): 769.
60. Semchuk O.Y., Biliuk A.A., Havryliuk O.O., Biliuk A.I. Kinetic theory of electroconductivity of metal nanoparticles in the condition of surface plasmon resonance. *Appl. Surf. Sci. Adv.* 2021. **3**: 100057.
61. Havryliuk O.O., Evtukh A.A., Pylypova O.V., Semchuk O.Y., Ivanov I.I., Zabolotnyi V.F. Plasmonic enhancement of light to improve the parameters of solar cells. *Appl. Nanosci.* 2020. **10**(12): 4759.
62. Zolotarenko O.D., Rudakova E.P., Zolotarenko A.D., Akhanova N.Y., Ualkhanova M.N., Shchur D.V., Gabdullin M.T., Gavrylyuk N.A., Myronenko T.V., Zolotarenko A.D., Chymbai M.V., Zagorulko I.V., Tarasenko Yu.O., Havryliuk O.O. Platinum-containing carbon nanostructures for the creation of electrically conductive ceramics using 3D printing of CJP technology. *Him. Fiz. Tehnol. Poverhni*. 2022. **13**(3): 259.
63. Zolotarenko Ol.D., Rudakova E.P., Akhanova N.Y., Zolotarenko An.D., Shchur D.V., Gabdullin M.T., Ualkhanova M., Sultangazina M., Gavrylyuk N.A., Chymbai M.V., Zolotarenko A.D., Zagorulko I.V., Tarasenko Yu.O. Plasmochemical Synthesis of Platinum-Containing Carbon Nanostructures Suitable for CJP 3D-Printing. *Metallophysics and Advanced Technologies*. 2022. **44**(3): 343.
64. Zolotarenko Ol.D., Rudakova E.P., Akhanova N.Y., Zolotarenko An.D., Shchur D.V., Gabdullin M.T., Ualkhanova M., Gavrylyuk N.A., Chymbai M.V., Myronenko T.V., Zagorulko I.V., Zolotarenko A.D., Havryliuk O.O. Electrically conductive composites based on TiO_2 and carbon nanostructures manufactured using 3D printing of CJP technology. *Him. Fiz. Tehnol. Poverhni*. 2022. **13**(4): 415.

65. Zolotarenko Ol.D., Rudakova E.P., Akhanova N.Y., Zolotarenko An.D., Shchur D.V., Gabdullin M.T., Ualkhanova M., Gavrylyuk N.A., Chymbai M.V., Tarasenko Yu.O., Zagorulko I.V., Zolotarenko A.D. Electric Conductive Composites Based on Metal Oxides and Carbon Nanostructures. *Metallophysics and Advanced Technologies.* 2021. **43**(10): 1417.
66. Stavitskaya S.S., Mironyuk T.I., Kartel M.T., Strelko V.V. Sorption characteristics of "food fibers" in secondary products of processing of vegetable raw materials. *Russ. J. Appl. Chem*. 2001. **74**(4): 592.
67. Zakutevskii O.I., Psareva T.S., Strelko V.V., Kartel M.T. Sorption of U(VI) from aqueous solutions with carbon sorbents. *Radiochemistry*. 2007. **49**(1): 67.
68. Kartel M., Galysh V. New composite sorbents for caesium and strontium ions sorption. *Chemistry Journal of Moldova*. 2017. **12**(1): 37.
69. Gun'ko V.M., Turov V.V., Protsak I.S., Krupska T.V., Pakhlov E.M., Tsapko M.D. Effects of pre-adsorbed water on methane adsorption onto blends with hydrophobic and hydrophilic nanosilicas. *Colloids Surf A*. 2019. **570**: 471.
70. Galysh V., Sevastyanova O., Kartel M., Lindström M.E., Gornikov Y. Impact of ferrocyanide salts on the thermo-oxidative degradation of lignocellulosic sorbents. *J. Therm. Anal. Calorim*. 2017. **128**(2): 1019.
71. Ivashchenko V.I., Turchi P.E.A., Shevchenko V.I., Ivashchenko L.A., Rusakov G.V. Atomic and electronic structures of a-SiC:H from tight-binding molecular dynamics. *J. Phys.: Condens. Matter*. 2003. **15**(24): 4119.
72. Gabdullin M.T., Khamitova K.K., Ismailov D.V., Sultangazina M.N., Kerimbekov D.S., Yegemova S.S., Chernoshtan A., Schur D.V. Use of nanostructured materials for the sorption of heavy metals ions. *IOP Conf. Ser.: Mater. Sci. Eng*. 2019. **511**(1): 12044.
73. Gun'ko V.M., Lupascu T., Krupska T.V., Golovan A.P., Pakhlov E.M., Turov V.V. Influence of tannin on aqueous layers at a surface of hydrophilic and hydrophobic nanosilicas. *Colloids Surf. A*. 2017. **531**: 9.
74. Sementsov Yu.I., Prikhod'ko G.P., Melezhik A.V., Aleksyeyeva T.A., Kartel M.T. Physicochemical properties and biocompatibility of polymer/carbon nanotubes composites. In: *Nanomaterials and Supramolecular Structures*. 2010. P. 347.
75. Khamitova K.K., Kayupov B.A., Yegemova S.S., Gabdullin M.T., Abdullin Kh.A., Ismailov D.V., Kerimbekov D.S. The use of fullerenes as a biologically active molecule. *Int. J. Nanotechnol*. 2019. **16**(1–3): 100.
76. Gun'ko V.M., Turov V.V., KrupskaT.V., Tsapko M.D. Interactions of human serum albumin with doxorubicin in different media. *Chem. Phys.* 2017. **483**–**484**: 26.
77. Krupska T.V., Turova A.A., Un'Ko V.M., Turov V.V. Influence of highly dispersed materials on physiological activity of yeast cells. *Biopolymers and Cell*. 2009. **25**(4): 290.
78. Savenko A.F., Bogolepov V.A., Meleshevich K.A., Zaginaichenko S.Yu., Lototsky M.V., Pishuk V.K., Teslenko L.O., Skorokhod V.V. Structural and methodical features of the installation for the investigations of hydrogen-sorption characteristics of carbon nanomaterials and their composites. *NATO Security through Science Series A: Chemistry and Biology*. 2007: 365.
79. Zaginaichenko S., Nejat Veziroglu T. Peculiarities of hydrogenation of pentatomic carbon molecules in the frame of fullerene molecule C_{60}. *Int. J. Hydrogen Energy*. 2008. **33**(13): 3330.
80. Zaginaichenko S.Yu., Veziroglu T.N., Lototsky M.V., Bogolepov V.A., Savenko A.F. Experimental set-up for investigations of hydrogen-sorption characteristics of carbon nanomaterials. *Int. J. Hydrogen Energy*. 2016. **41**(1): 401.
81. Lakhnik A.M., Kirian I.M., Rud A.D. The Mg/MAX-phase composite for hydrogen storage. *Int. J. Hydrogen Energy*. 2022. **47**(11): 7274.
82. Schur D.V., Zaginaichenko S.Y., Savenko A.F., Bogolepov V.A., Anikina N.S., Zolotarenko A.D., Matysina Z.A., Veziroglu T.N., Skryabina N.E. Hydrogenation of fullerite C_{60} in gaseous phase. *NATO Science for Peace and Security Series C: Environmental Security*. 2011. **2**: 87.
83. Matysina Z.A. Phase transformations $\alpha \rightarrow \beta \rightarrow \gamma \rightarrow \delta \rightarrow \varepsilon$ in titanium hydride tihx with increase in hydrogen concentration. *Russ. Phys. J.* 2001. **44**(11): 1237.
84. Lyashenko A.A., Adejev V.M., Voitovich V.B., Zaginaichenko S.Yu. Niobium as a construction material for a hydrogen energy system. *Int. J. Hydrogen Energy*. 1995. **20**(5): 405.
85. Lavrenko V.A., Adejev V.M., Kirjakova I.E. Studies of the hydride formation mechanism in metals. *Int. J. Hydrogen Energy*. 1994. **19**(3): 265.
86. Zaginaichenko S.Y., Matysina Z.A., Teslenko L.O., Veziroglu A. The structural vacancies in palladium hydride. Phase diagram. *Int. J. Hydrogen Energy*. 2011. **36**(1): 1152.
87. Bogolepov V.A., Veziroglu A., Zaginaichenko S.Y., Savenko A.F., Meleshevich K.A. Selection of the hydrogen-sorbing material for hydrogen accumulators. *Int. J. Hydrogen Energy*. 2016. **41**(3): 1811.

88. Shchur D.V., Zaginaichenk S.Y., Veziroglu A., Veziroglu T.N., Gavrylyuk N.A., Zolotarenko A.D., Gabdulli M.T., Ramazanov T.S., Zolotarenko A.D., Zolotarenko A.D. Prospects of Producing Hydrogen-Ammonia Fuel Based on Lithium Aluminum Amide. *Russ. Phys. J*. 2021. **64**(1): 89.
89. Trefilov V.I., Pishuk V.K., Zaginaichenko S.Yu., Choba A.V., Nagornaya N.R. Solar furnaces for scientific and technological investigation. *Renewable energy*. 1999. **16**(1–4 pt 2): 757.
90. Matysina Z.A., Gavrylyuk N.A., Kartel M., Veziroglu A., Veziroglu T.N., Pomytkin A.P., Schur D.V., Ramazanov T.S., Gabdullin M.T., Zolotarenko A.D., Zolotarenko A.D., Shvachko N.A. Hydrogen sorption properties of new magnesium intermetallic compounds with $MgSnCu_4$ type structure. *Int. J. Hydrogen Energy*. 2021. **46**(50): 25520.
91. Matysina Z.A., Pogorelova O.S., Zaginaichenko S.Yu. The surface energy of crystalline CuZn and FeAl alloys. *J. Phys. Chem. Solids*. 1995. **56**(1): 9.
92. Rud A.D., Schmidt U., Zelinska G.M., Lakhnik A.M., Kolbaso G.Ya., Danilov M.O. Atomic structure and hydrogen storage properties of amorphous-quasicrystalline Zr-Cu-Ni-Al melt-spun ribbons. *J. Non-Cryst. Solids*. 2007. **353**(32–40): 3434.
93. Matysina Z.A., Zaginaichenko S.Yu. Hydrogen solubility in alloys under pressure. *Int. J. Hydrogen Energy*. 1996. **21**(11–12): 1085.
94. Zaginaichenko S.Yu., Matysina Z.A., Smityukh I., Pishuk V.K. Hydrogen in lanthan-nickel storage alloys. *J. Alloys Compd*. 2002. **330–332**: 70.
95. Lytvynenko Yu.M. Utilization the concentrated solar energy for process of deformation of sheet metal. *Renewable Energy*. 1999. **16**(1–4): 753.
96. Matysina Z.A., Zaginaichenko S.Y. Sorption Properties of Iron–Magnesium and Nickel–Magnesium Mg_2FeH_6 and Mg_2NiH_4 Hydrides. *Russ. Phys. J.* 2016. **59**(2): 177.
97. Rud A.D., Schmidt U., Zelinska G.M., Lakhnik A.M., Perekos A.E., Kolbasov G.Ya., Danilov M.O. Peculiarities of structural state and hydrogen storage properties of Ti-Zr-Ni based intermetallic compounds. *J. Alloys Compd*. 2005. **404–406**(SPEC. ISS.): 515.
98. Tikhotskii S.A., Fokin I.V. Traveltime seismic tomography with adaptive wavelet parameterization. *Izvestiya Phys. Solid Earth*. 2011. **47**(4): 327.
99. Zaginaichenko S.Y., Zaritskii D.A., Matysina Z.A., Veziroglu T.N., Kopylova L.I. Theoretical study of hydrogen-sorption properties of lithium and magnesium borocarbides. *Int. J. Hydrogen Energy*. 2015. **40**(24): 7644.
100. Matysina Z.A., Zaginaichenko S.Y. Hydrogen-sorption properties of magnesium and its intermetallics with Ca_7Ge-Type structure. *Phys. Met. Metall*. 2013. **114**(4): 308.
101. Kryvoglaz M.A. Solubility in ordering alloys. *Journal of Technical Physics*. 1954. **24**: 1077.
102. Matysina Z.A., Zolonarenko An.D., Zolonarenko Al.D., Gavrylyuk N.A., Veziroglu A., Veziroglu T.N., Gabdullin M.T., Pomytkin A.P., Schur D.V. *Features of the interaction of hydrogen with metals, alloys and compounds. (Hydrogen atoms in crystalline solids).* (Kyiv: Publishing House "KIM", 2022).
103. Krivoglaz M.A., Smirnov A.A. *Theory of ordered alloys*. (Moscow: Fizmatgiz, 1958). [in Russian].

Received 02.03.2023, accepted 05.06.2023